Analysis of an Airfoil by Changing the Size, Shape and Location of the Dimple

Arvind Mukundan

Abstract:- It has been found that by placing a dimple in an aerofoil will reduce drag at a specific AOA. This project work illustrates the change in aerodynamic characteristics of an airfoil by changing the size, shape and location of dimples in an aerofoil. By considering numerous types of dimples, alterations have been done and studied at different Angle of Attacks. Aerodynamic analysis for this airfoil is carried out using Computational Fluid Dynamics. From this investigation it has been detected that the lift force and stall Angle of Attack has been increased efficiently by simply using dimples on the aerofoil.

I. INTRODUCTION

Over the past decade, various aerodynamic simulation has been conducted which provide insights of complex flows and to provide design inputs [2]. Various aerodynamic simulations have been conducted on sports balls [3]. For example, one of the research works is to analyze the basic aerodynamic characteristics of conventional volleyballs and new volleyballs by using a wind tunnel [4]. On the other hand, many research works have been conducted on golf balls [5] [6] [7]. On analyzing the golf ball, the aerodynamics present in the dimple over the ball results in experiencing drag force smaller than the smooth surfaced ball. In a golf ball, non-circular isodiametric dimples provide increased efficiency of coverage of the surface of a golf ball. Additionally, the aerodynamic properties of the ball are improved [8]. In deep, dimples delay the flow separation point by creating turbulent boundary layer by reenergizing potential energy in

to kinetic energy. Modifying the aircraft wing structure by means of placing dimples will reduce the drag to considerable amount from the total drag and helps to stabilize the aircraft during stall [9]. Turbulence can be caused due to the introduction of dimples on the aircraft wing by creating vortices delaying the boundary layer separation eventually reducing the pressure drag and raise in the stall angle [10]. Also, the inward dimples are more effective than the outward dimples for cases where the dimples were seen effective [11] while the wake region, increases the pressure drag at higher angle of attack which is due to flow separation [12].

II. GEOMETRY DESIGN

The reason for choosing a semi spherical dimple is that it is a bluff body, so when placed in a flow separation regime, it would gain some turbulent kinetic energy to stick to the surface thereby reducing the pressure drag. The geometry is drawn using CATIA. Once the airfoil is imported, the control volume (Domain) surrounding the airfoil is drawn by taking the considerations of making it 15 times greater than the chord length (1m). The semi spherical dimple is placed at two points 20% of chord length and 40% of chord length. The reason for choosing these points is that these are just ahead and behind the maximum thickness point, from where the flow separation might take place. The dimple is drawn to the radius of 20mm. The comparative study is done between the normal airfoil and the ones with the dimple for a angle of attack.
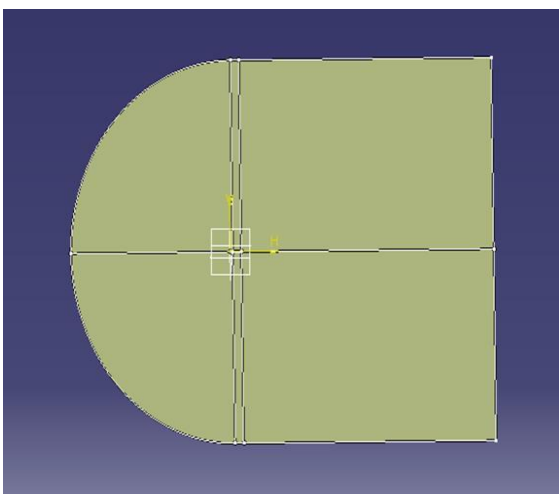

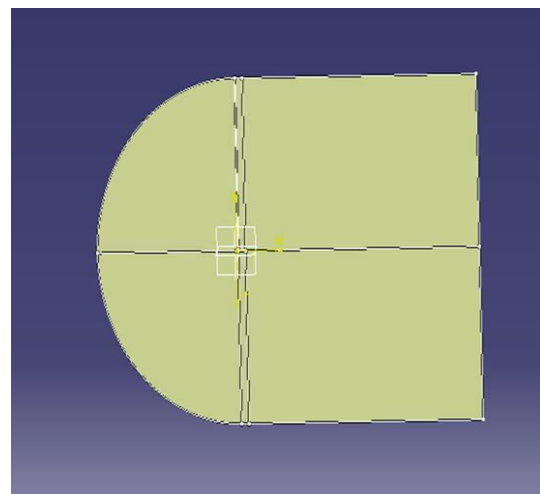Fig 1:- Domain for normal airfoil using CATIA

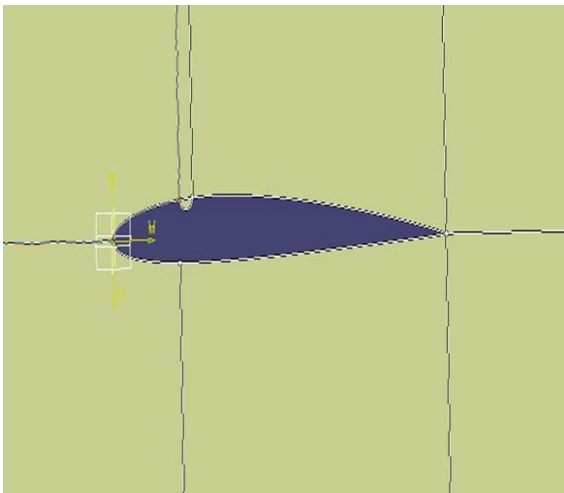Fig 2:- Domain for dimpled airfoil using CATIA
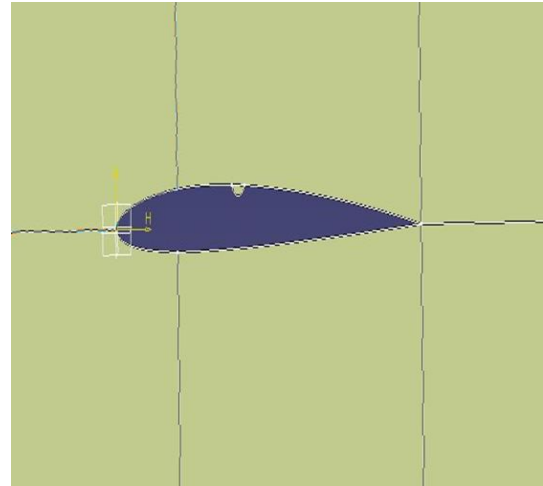
Fig 3:- Dimple at 20% chord length

Fig 4:- Dimple at 20% chord length

III.   ANALYSIS PARAMETERS

A parameter, generally, is any characteristic that can help in defining or classifying a system. A parameter is an element of a system that is useful, or critical, when identifying the system, or when evaluating its performance, status, condition, etc. Here, we have the following parameters,

➢ *AIRFOIL SPECFICATIONS*

S.NO	PARAMETER	VALUES
1	CHORD LENGTH	1m
2	DIMPLE RADIUS	0.02m
3	SERIES CODE	NACA 2412
4	EXPERIMENTAL AOA	0,5,8,12,17,19,20,21 (degrees)
5	MATERIAL	Solid Aluminum

Table 1

➢ *BOUNDARY CONDITIONS:*

A condition that is required to be satisfied at all or part of the boundary of a region in which a set of differential conditions is to be solved. They are given in order to satisfy the required external factors and conditions and make the experimental atmosphere like the original atmosphere where the process takes place.

➢ *INITIAL BOUNDARY CONDITIONS*

PARAMETER	VALUES
INLET VELOCITY	100 m/s
PRESSURE	1 atm
DENSITY	1.225 kg/m3
REYNOLDS NUMBER	6177509
FLUID	Air

Table 2

The domain for the airfoil is already created for the airfoil using CATIA.
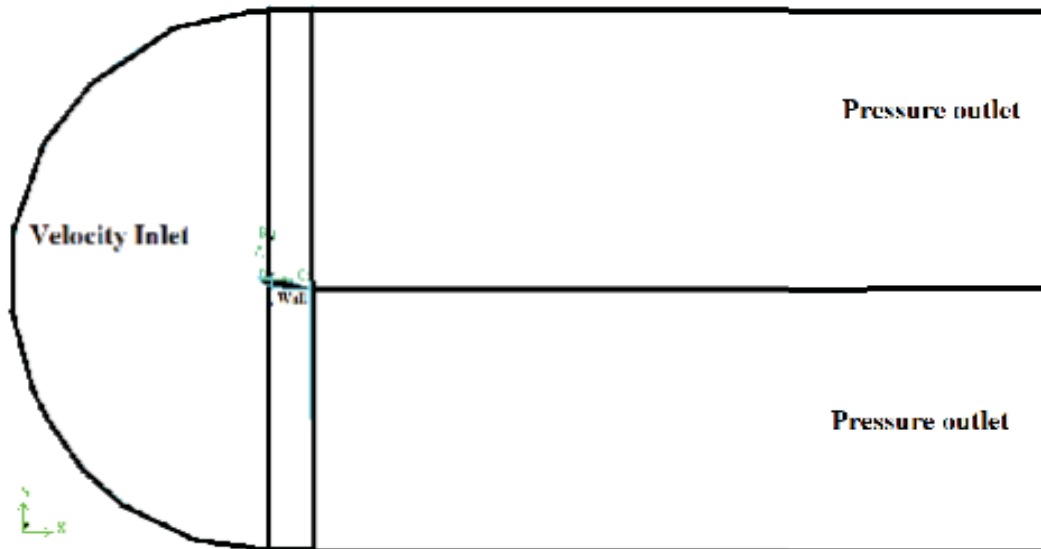
Fig. 5:- Boundary Conditions for post processing

➢ *MESHING*

It is the process of representing a geometric object as a set of finite elements for analysis. It is one of the most important and crucial processes in ANSYS.

➢ *PROCEDURE:*

● Initially the 2D diagram is analyzed for the number of profiles.
● Each profile is meshed along its edge using the edge size meshing tool.
● A maximum number of divisions of 200 is given on each profile.
● Biasing is done systematically towards the airfoil wall, which makes it more concentrated towards the leading edge and the trailing edge.
● A bias factor of 20 is used is each case.
● Biasing is only given to the profiles on the peripheral surfaces of the airfoil.
● All the surfaces are mapped to the mesh and generated.
● Care must be taken to limit the minimum size of the divisions to ensure smooth meshing. Usually the minimum size is of the order of 10^{-4}.

➢ *MESHING CONDITIONS*

S.NO	PARAMETERS	VALUES / CONDITIONS
1	Minimum size of mesh	6.6667 x 10-4 m
2	Maximum size of mesh	0.1224 x 10-2 m
3	Bias factor	20
4	Number of profiles (Plain, 20%, 40%)	18, 20, 20
5	Number of surfaces (Plain, 20%, 40%)	6, 8 ,8

Table 3
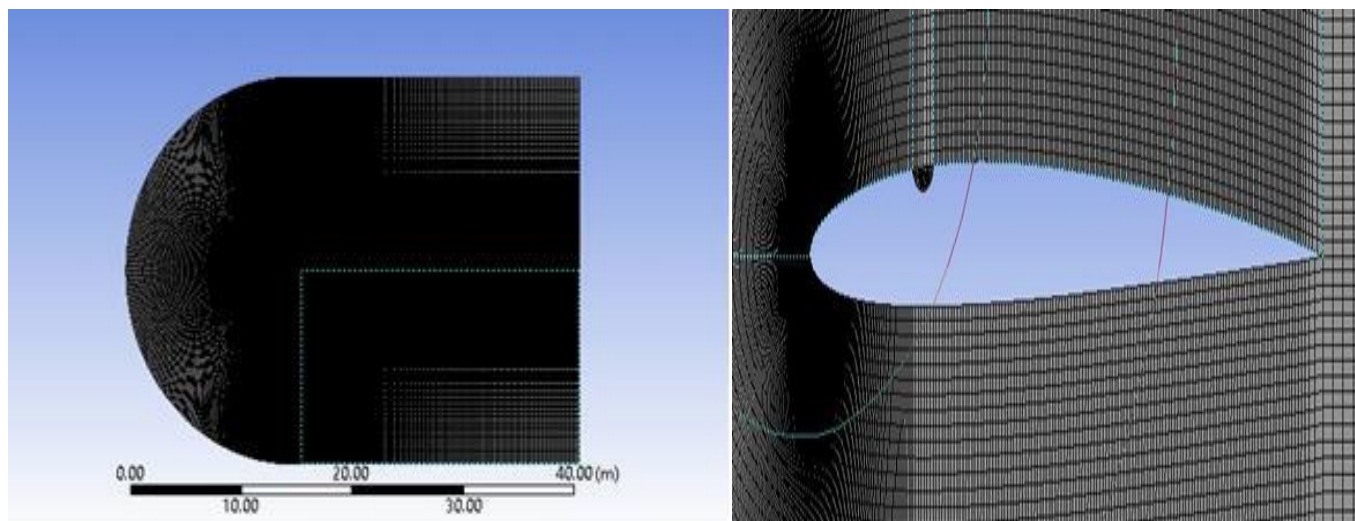
Fig. 6,7 :- Entire domain mesh and Meshing for airfoil view for dimple at 20% chord length
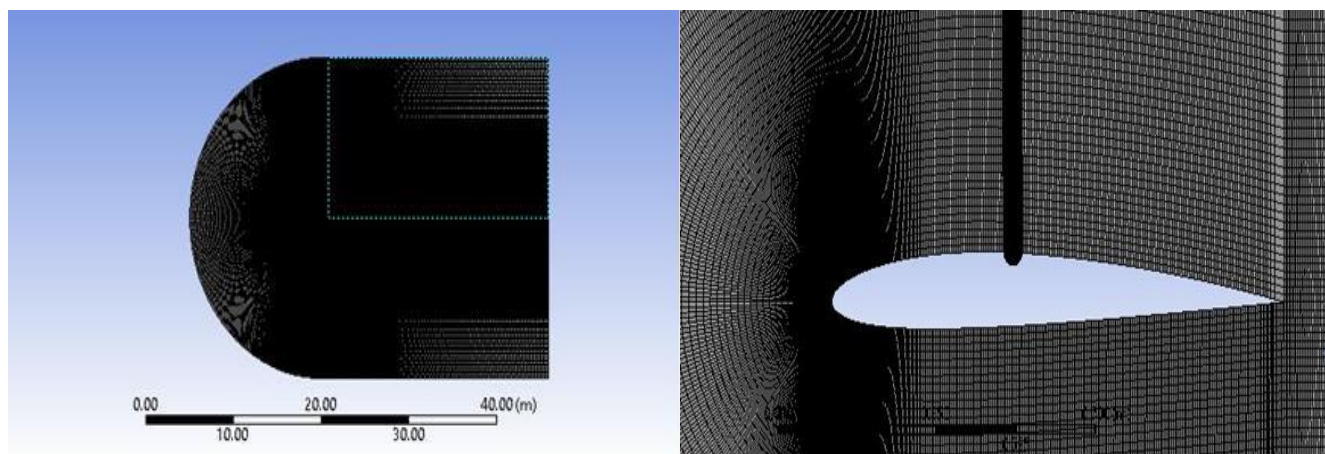
Fig. 8, 9 :- Entire domain mesh and Meshing for airfoil view for dimple at 40% chord length

➢ *CALCULATIONS AND ANALYSIS*
    Various calculation parameters and values are required to obtain the accurate result. The various input required for analysis are, INPUT PARAMETERS

S.NO	PARAMETERS	VALUES/CONDITIONS
1	Inlet velocity	100m/s(x direction)
2	Pressure	1 atm
3	Gradient	Least squares cell based
4	Pressure	Second order
5	Momentum	First order upwind
6	Turbulent kinetic energy	First order upwind
7	Turbulent dissipation rate	
8	Number of iterations	1000
9	Calculation model	k-epsilon
10	plots	Cl_{l2} CD

Table 4

IV. RESULTS AND GRAPHS

6.1 OBSERVATION TABLE

NACA 2412 ANALYSIS (2D)

S.NO	ANGLE OF ATTACK DEGREES	TYPE	DISTANCE FROM TIP % OF CHORD	CL	CD	L/D	CL XFLR	CD XFLR	L/D XFLR
1	0	PLAIN	N/A	0.232	0.00623	37.23917	0.249	0.005	49.8
2	5			0.806	0.00788	102.2843	0.796	0.007	113.7143
3	8			0.989	0.00909	108.8009	1.127	0.009	125.2222
4	12			1.276	0.01211	105.3675	1.528	0.013	117.5385
5	17			1.659	0.02292	72.3822	1.83	0.025	73.2
6	19			1.7022	0.03622	46.99613	1.879	0.039	48.17949
7	20			1.6944	0.04511	37.56152	1.872	0.049	38.20408
8	21			1.6777	0.06384	26.27976	1.841	0.065	28.32308

S.NO	ANGLE OF ATTACK DEGREES	TYPE	DISTANCE FROM TIP % OF CHORD	CL	CD	L/D	CL PLAIN	CD PLAIN	L/D PLAIN
1	0	DIMPLE	20	0.189	0.00582	32.47423	0.232	0.00623	37.23917
2	5			0.638	0.00647	98.60896	0.806	0.00788	102.2843
3	8			0.887	0.00775	114.4516	0.989	0.00909	108.8009
4	12			1.273	0.0111	114.6847	1.376	0.01211	113.6251
5	17			1.595	0.02378	67.07317	1.659	0.02292	72.3822
6	19			1.738	0.04999	34.76695	1.7022	0.03622	46.99613
7	20			1.744	0.04844	36.0033	1.6944	0.04511	37.56152
8	21			1.722	0.066	26.09091	1.6777	0.06384	26.27976

S.NO	ANGLE OF ATTACK DEGREES	TYPE	DISTANCE FROM TIP % OF CHORD	CL	CD	L/D	CL PLAIN	CD PLAIN	L/D PLAIN
1	0	DIMPLE	40	0.182	0.00599	30.38397	0.232	0.00623	37.23917
2	5			0.554	0.00427	129.7424	0.806	0.00788	102.2843
3	8			0.774	0.0065	119.0769	0.989	0.00909	108.8009
4	12			1.2745	0.01107	115.131	1.376	0.01211	113.6251
5	17			1.4997	0.02858	52.47376	1.659	0.02292	72.3822
6	19			1.7779	0.03221	55.19714	1.7022	0.03622	46.99613
7	20			1.7922	0.0401	44.69327	1.6944	0.04511	37.56152
8	21			1.8033	0.05336	33.79498	1.6777	0.06384	26.27976
9	22			1.7802	0.07001	25.4278			

Table 5

PLOTS OF VELOCITY AT 0 AOA:
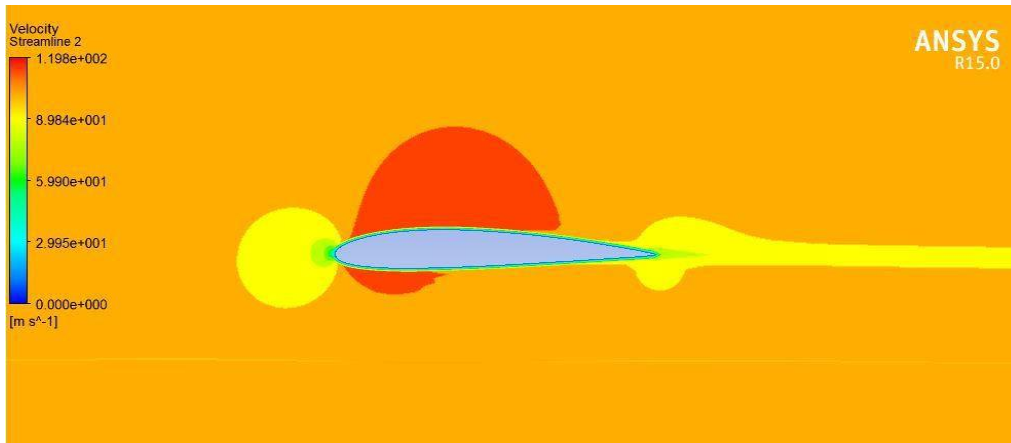
Fig.10:- Plain Airfoil at 0 AOA (V)
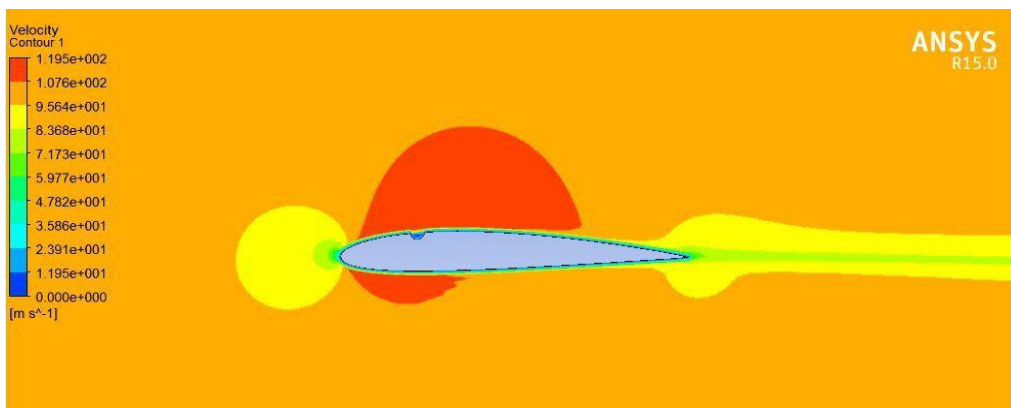
Fig.11:- Airfoil with dimple at 20% of chord length at 0 AOA (V)
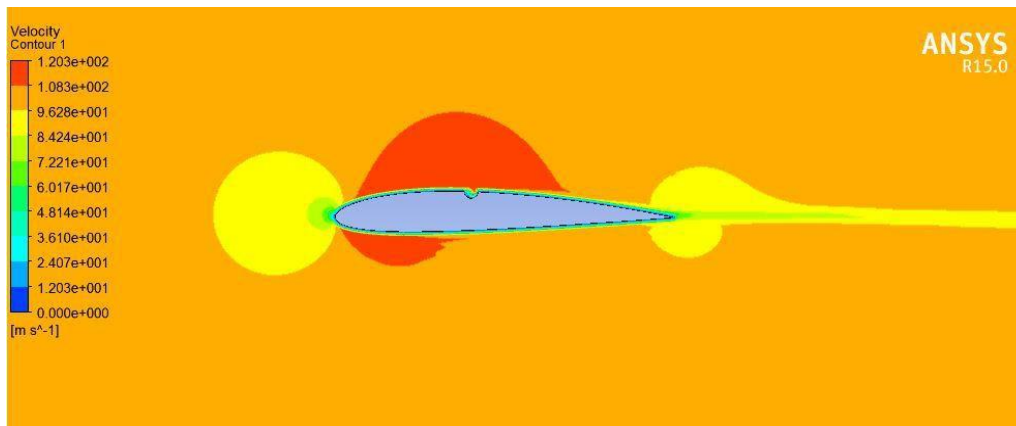
Fig.12:- Airfoil with dimple at 40% of chord length at 0 AOA (V)

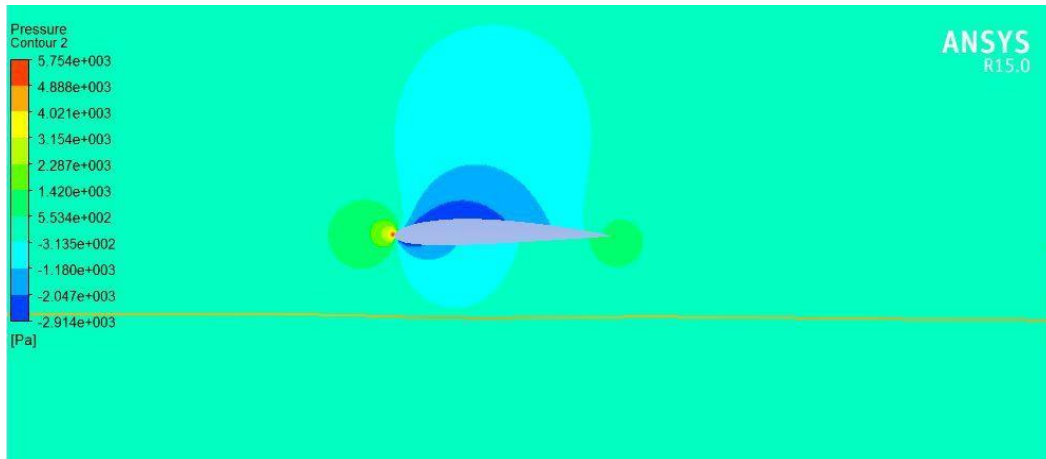## PLOTS OF STATIC PRESSURE AT 0 AOA:
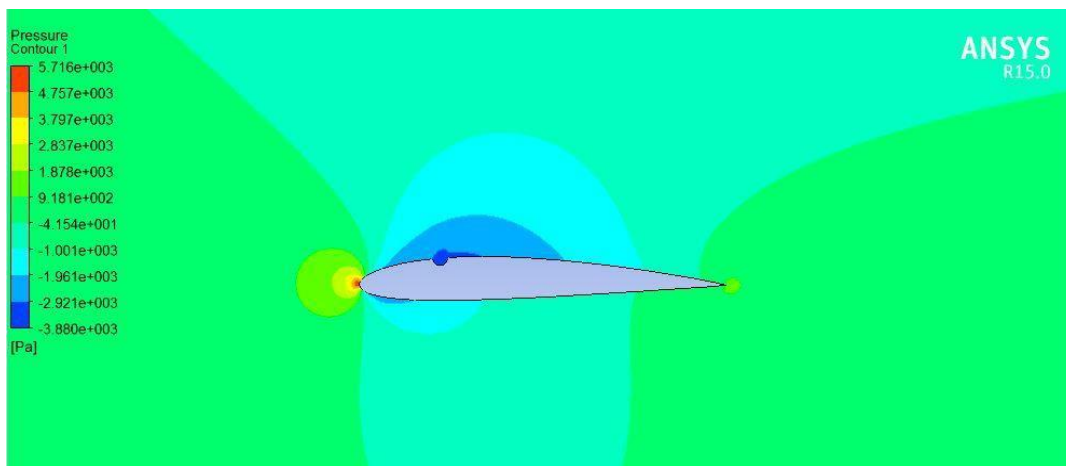

Fig.13 Plain Airfoil at 0 AOA (P)

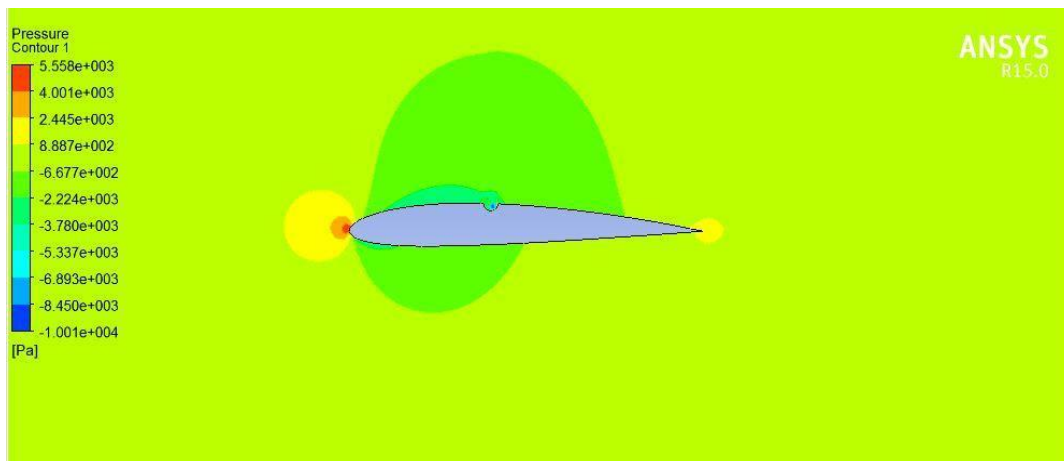Fig.14 Airfoil with dimple at 20% of chord length at 0 AOA (P)

Fig.15 Airfoil with dimple at 40% of chord length at 0 AOA (P)
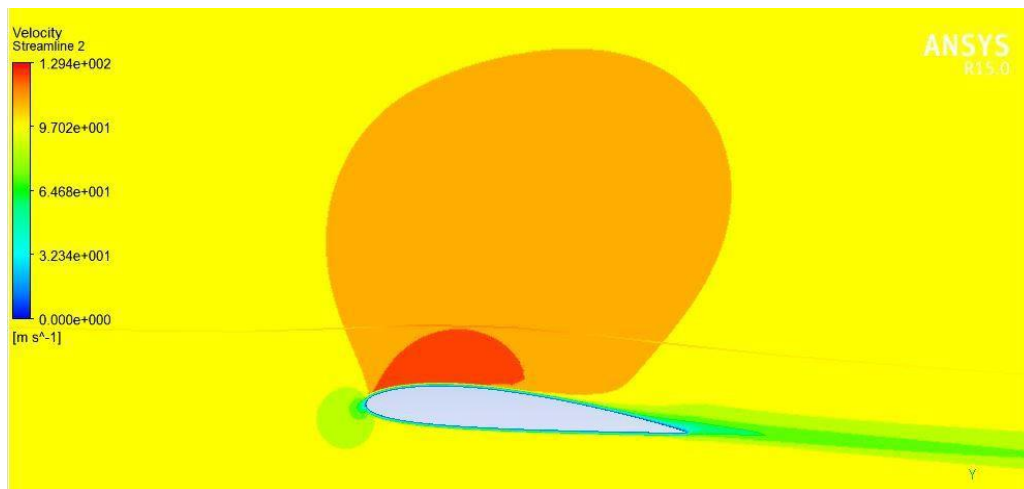
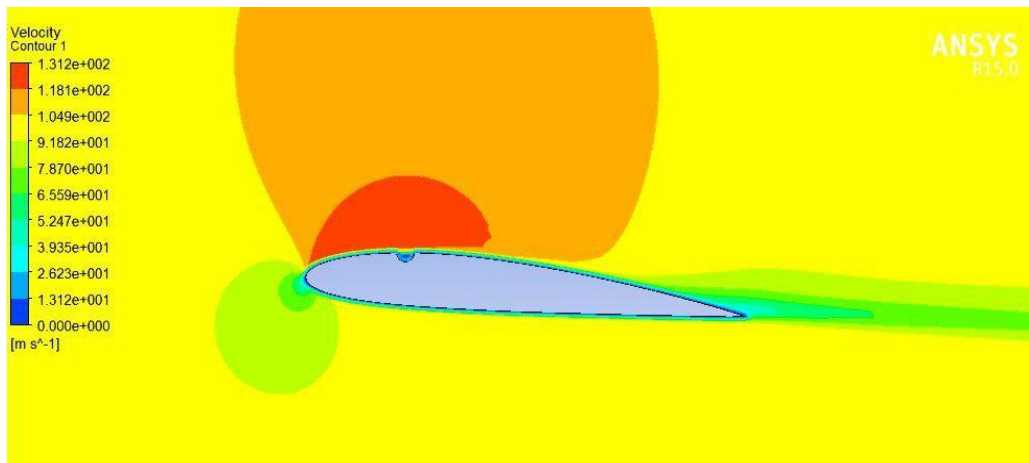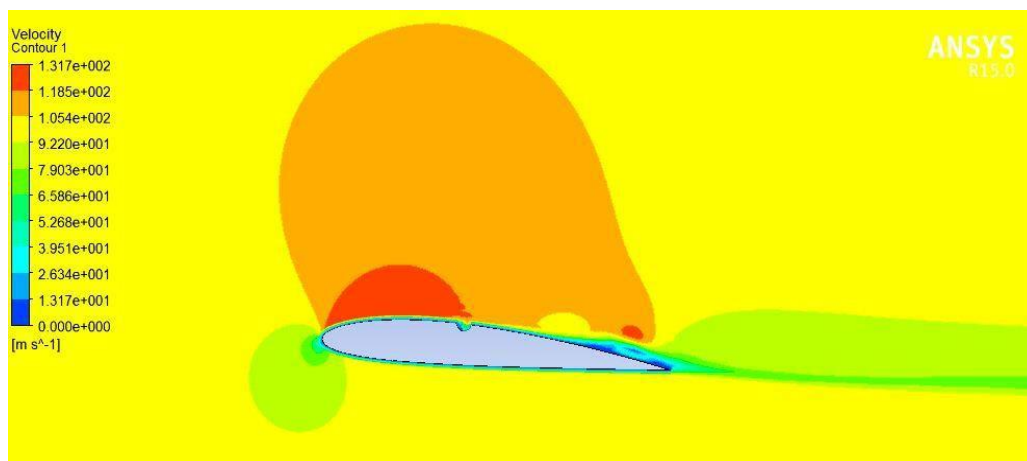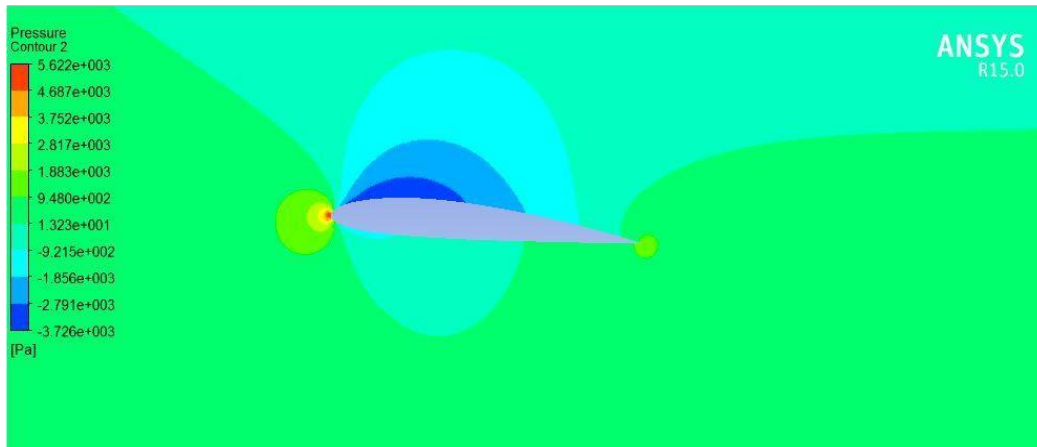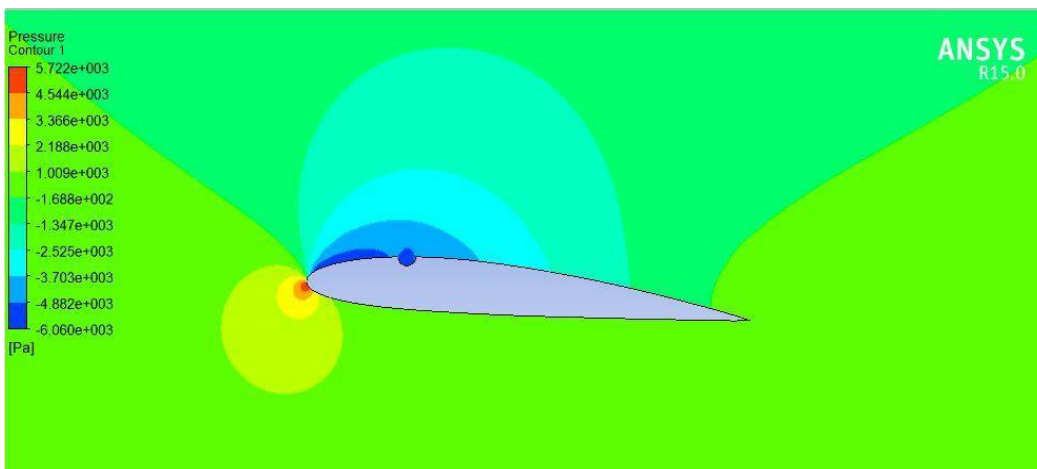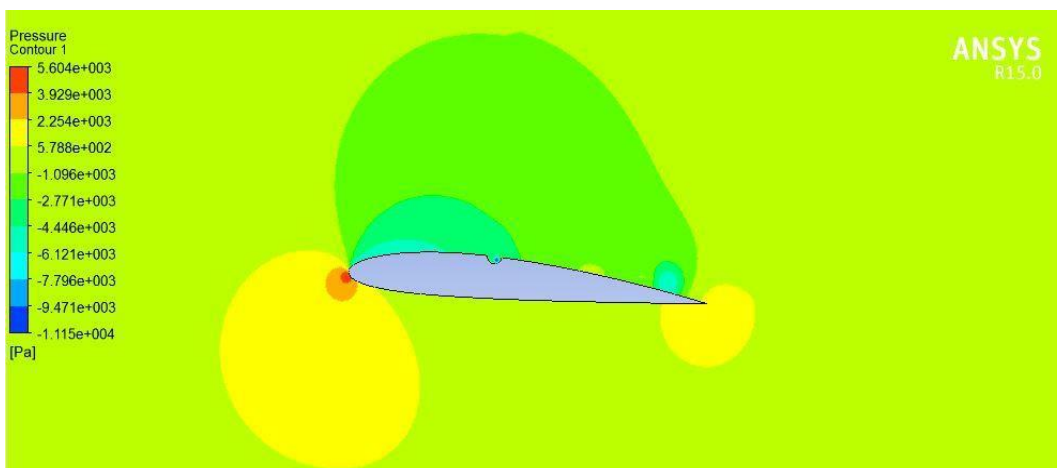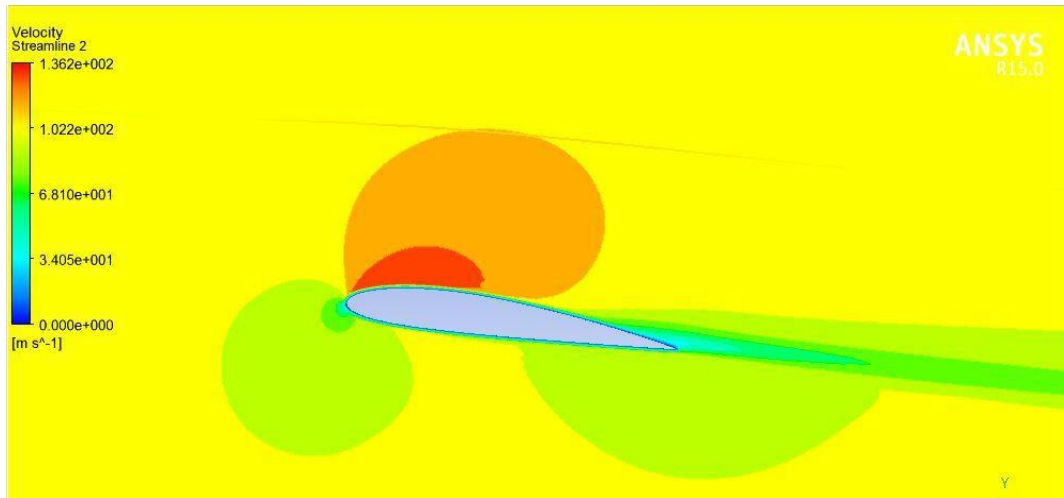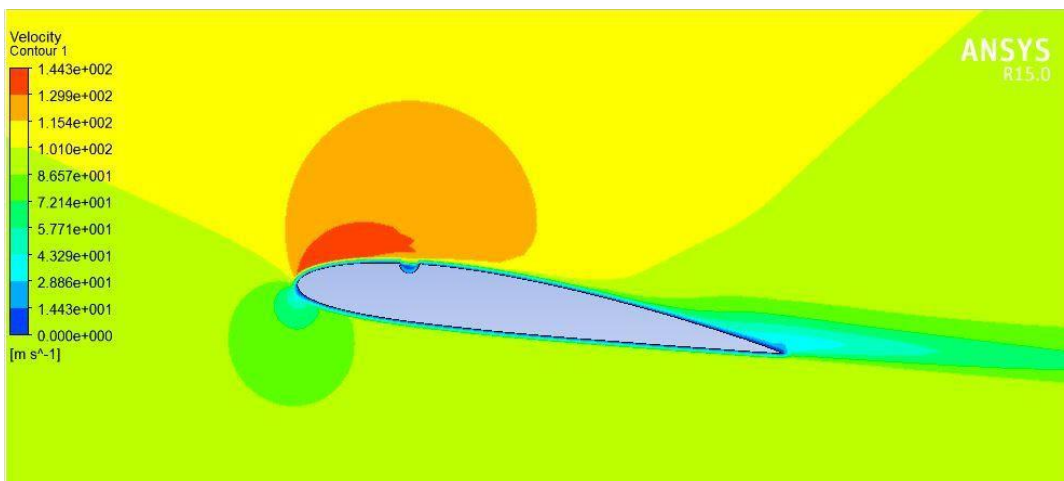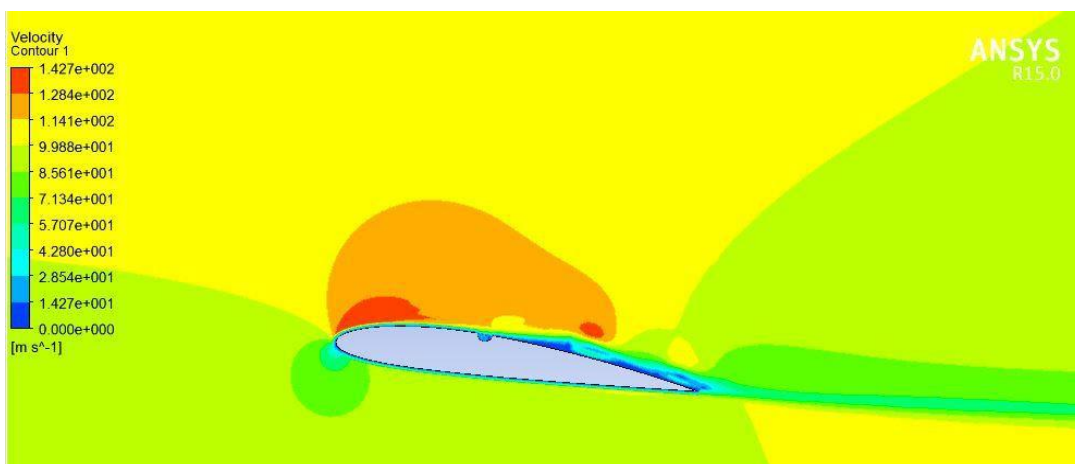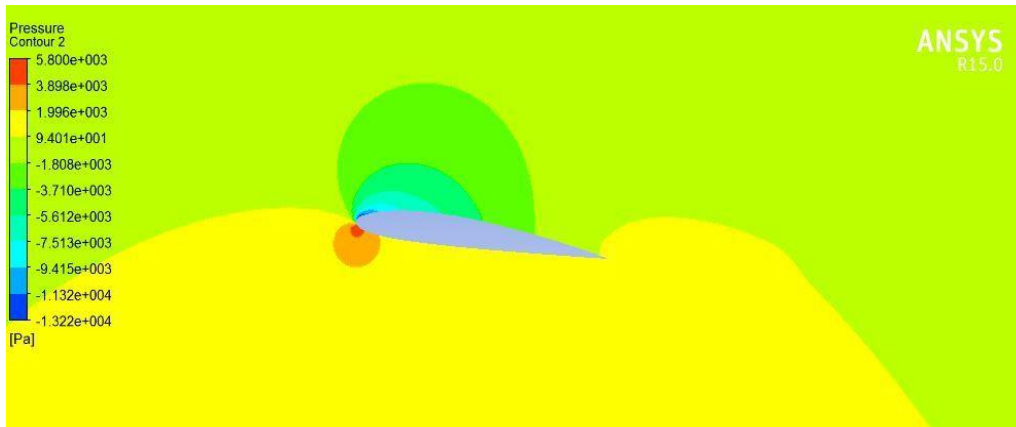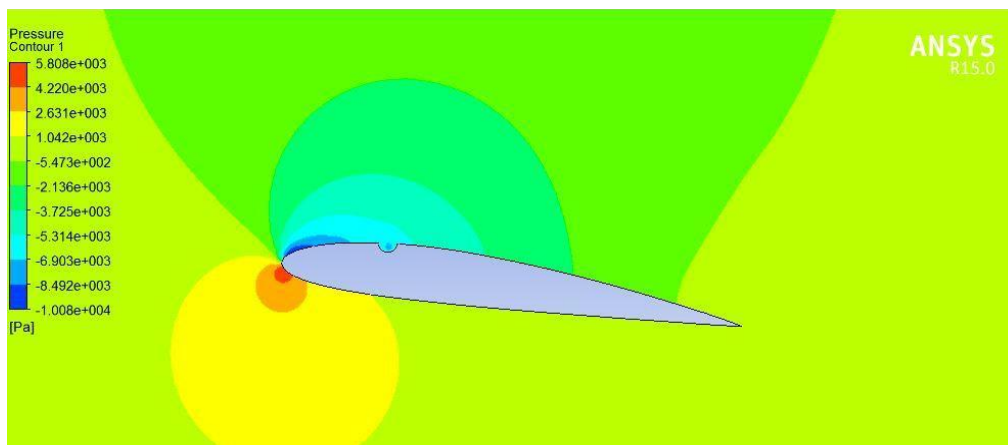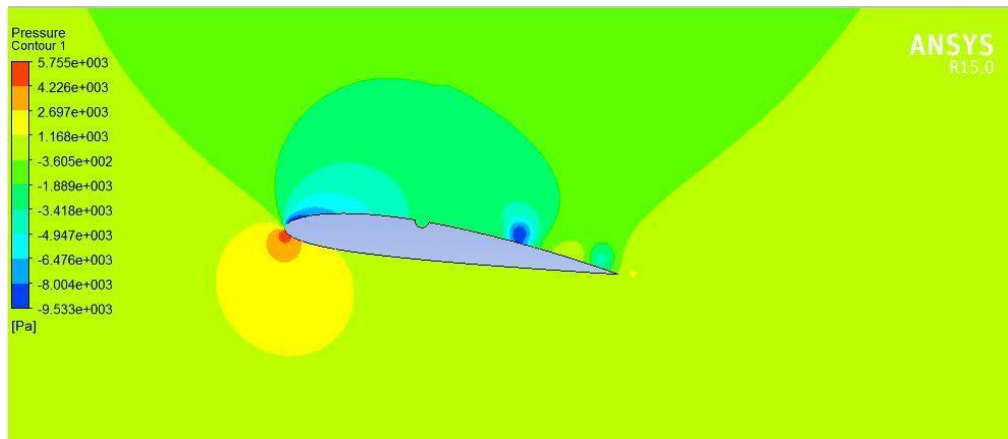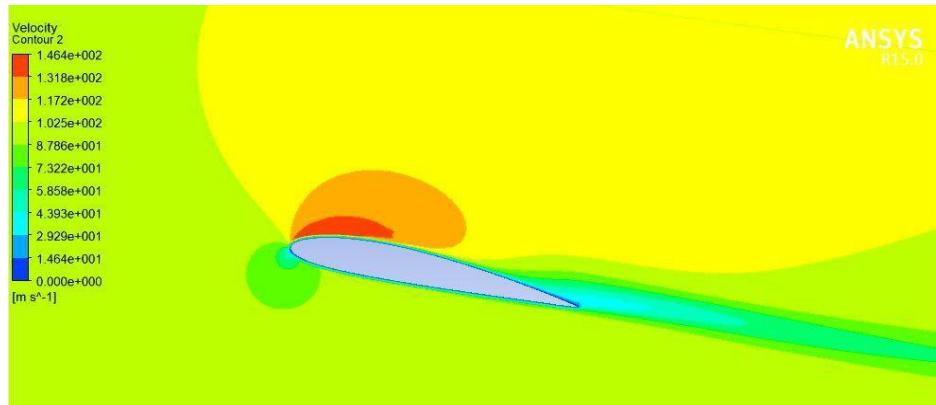**PLOTS OF VELOCITY AT 5 AOA:**
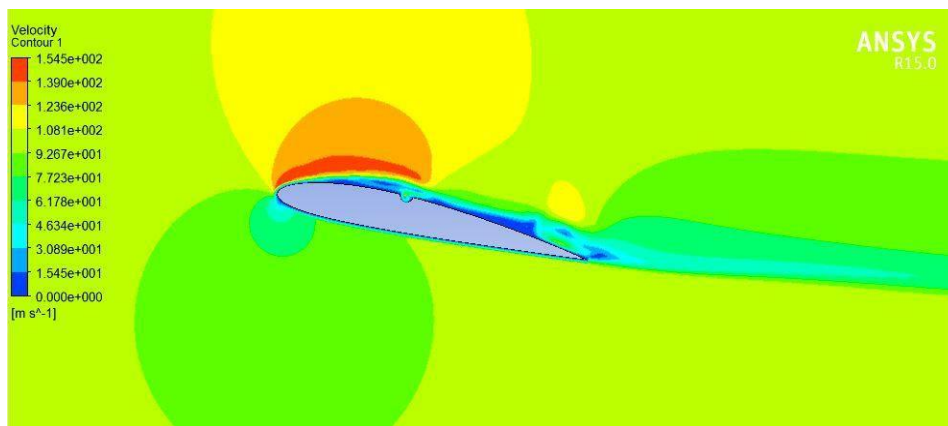

Fig.16 Plain Airfoil at 5 AOA (V)

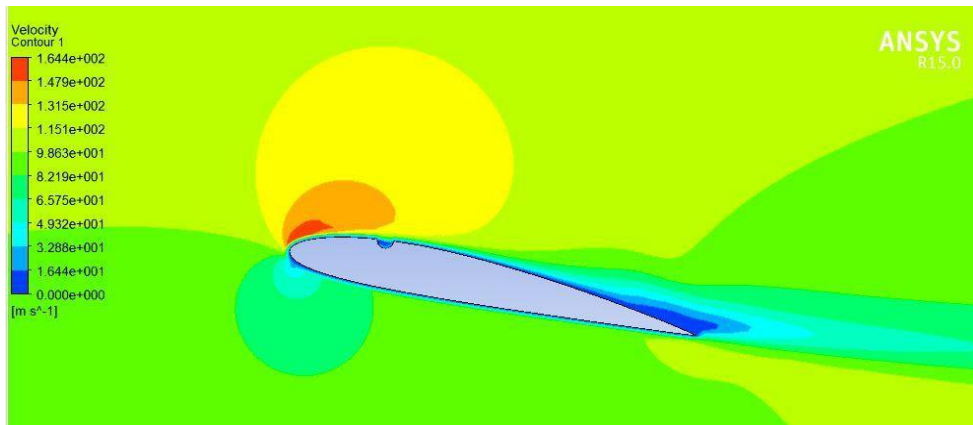Fig.17 Airfoil with dimple at 20% of chord length at 5 AOA (V)

Fig.18 Airfoil with dimple at 40% of chord length at 5 AOA (V)
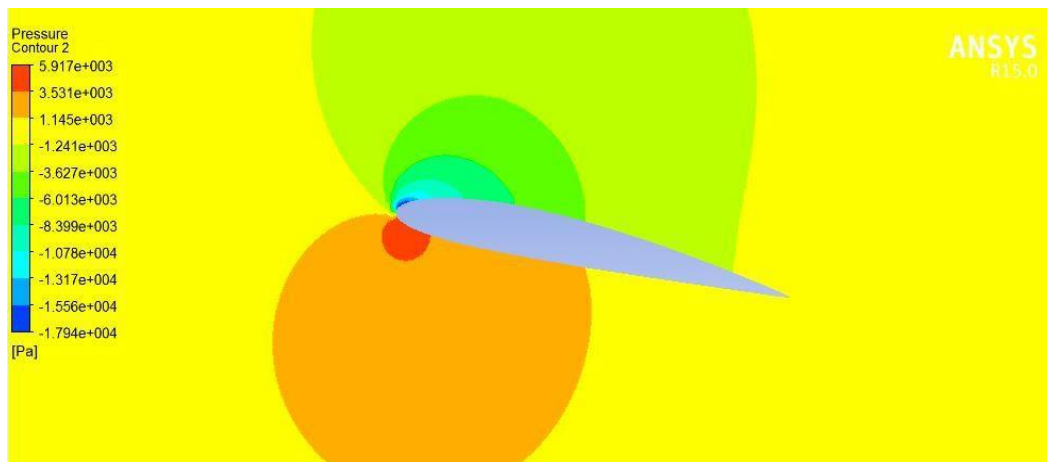
PLOTS OF STATIC PRESSURE AT 5 AOA:
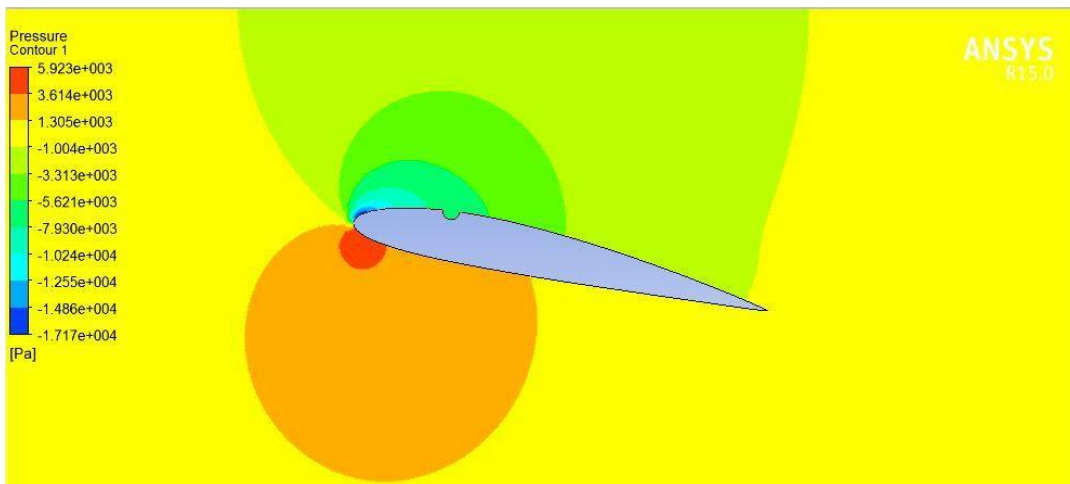

Fig.19 Plain Airfoil at 5 AOA (P)

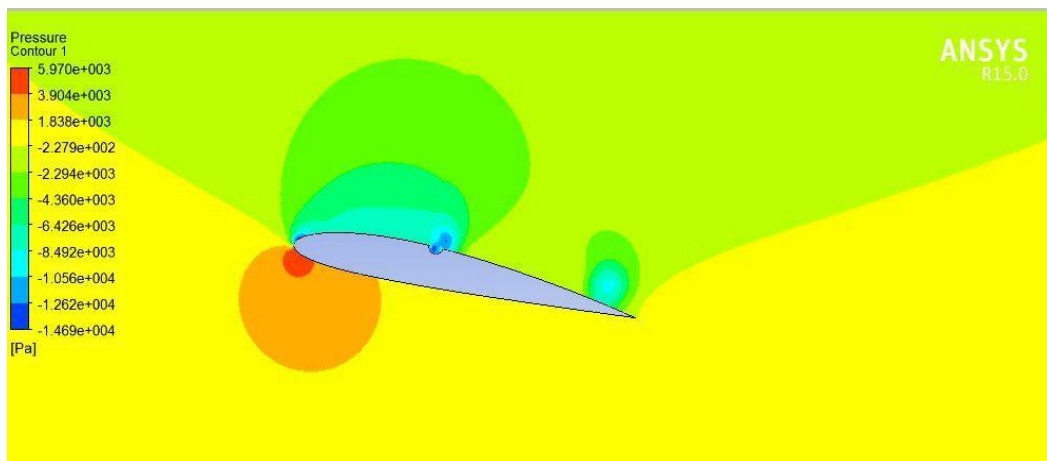Fig.20 Airfoil with dimple at 20% of chord length at 5 AOA (P)

Fig.21 Airfoil with dimple at 40% of chord length at 5 AOA (P)

PLOTS OF VELOCITY AT 8 AOA:

Fig.22 Plain Airfoil at 8 AOA (V)

Fig.23 Airfoil with dimple at 20% of chord length at 8 AOA (V)

Fig.24 Airfoil with dimple at 40% of chord length at 8 AOA (V)

PLOTS OF STATIC PRESSURE AT 8 AOA:

Fig.25 Plain Airfoil at 8 AOA (P)

Fig.26 Airfoil with dimple at 20% of chord length at 8 AOA (P)

Fig.27 Airfoil with dimple at 40% of chord length at 8 AOA (P)

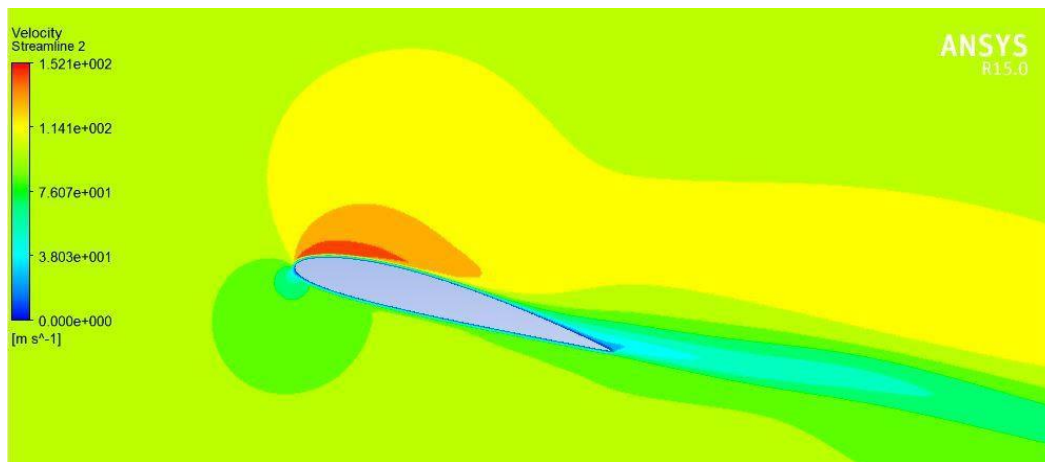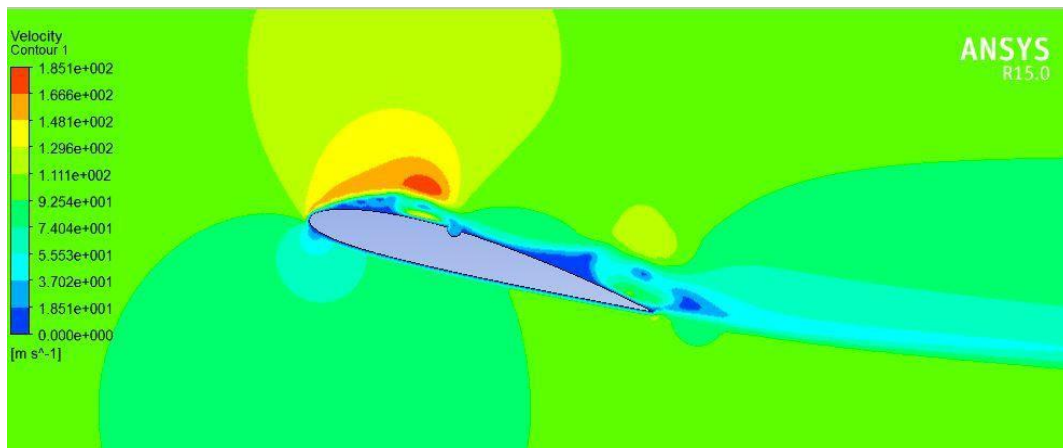**PLOTS OF VELOCITY AT 12 AOA:**

Fig.28 Plain Airfoil at 12 AOA (V)

Fig.29 Airfoil with dimple at 40% of chord length at 12 AOA (V)
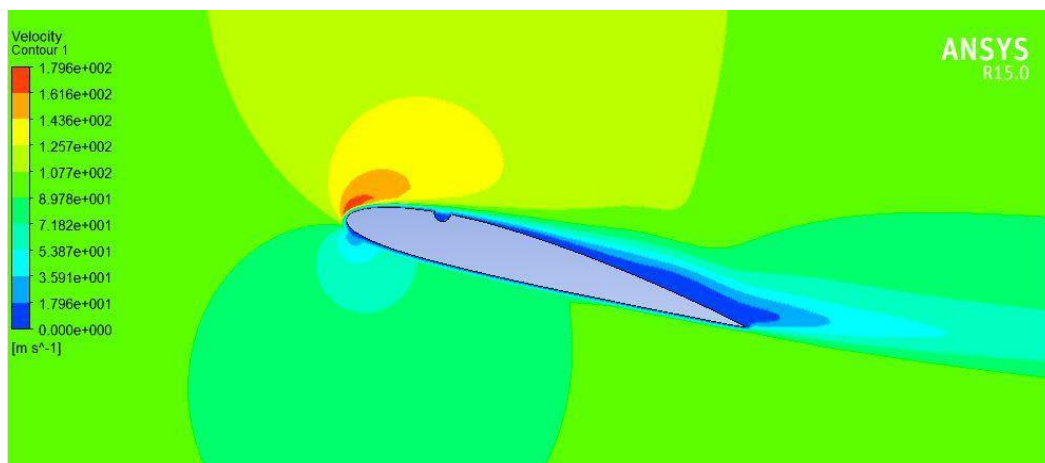

Fig.30 Airfoil with dimple at 20% of chord length at 12 AOA (V)
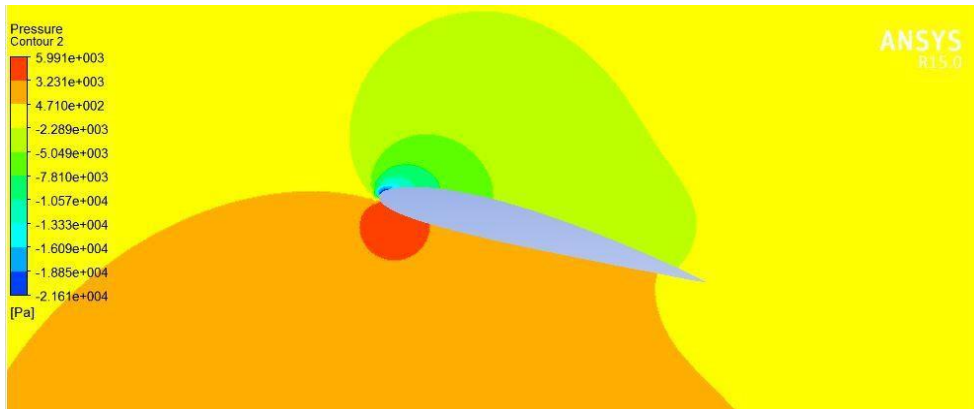
PLOTS OF STATIC PRESSURE AT 12 AOA:

Fig.31 Plain Airfoil at 12 AOA (P)

Fig.32 Airfoil with dimple at 20% of chord length at 12 AOA (P)

Fig.33 Airfoil with dimple at 40% of chord length at 12 AOA (P)

PLOTS OF VELOCITY AT 17 AOA:

Fig.34 Plain Airfoil at 17 AOA (V)

Fig.35 Airfoil with dimple at 40% of chord length at 17 AOA (V)

Fig.36 Airfoil with dimple at 20% of chord length at 17 AOA (V)

PLOTS OF STATIC PRESSURE AT 17 AOA:
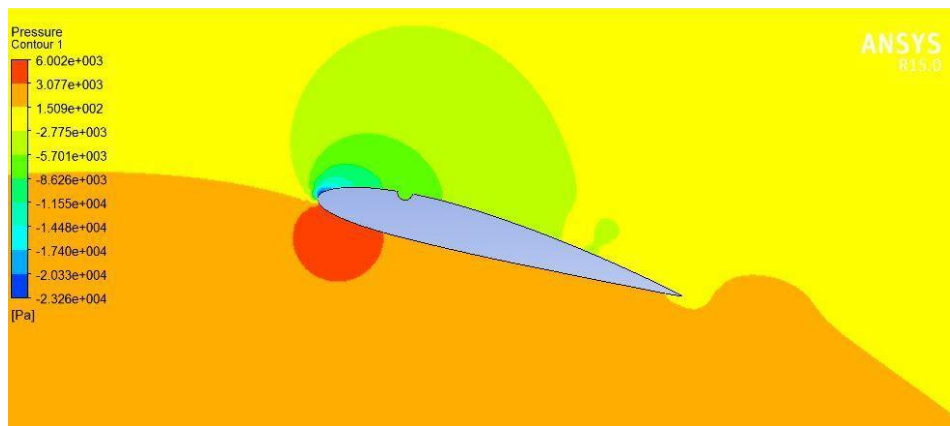

Fig.37 Plain Airfoil at 17 AOA (P)

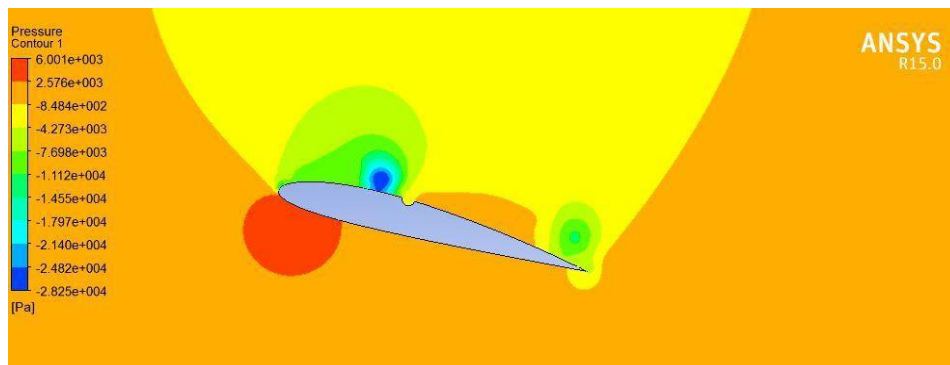Fig.38 Airfoil with dimple at 20% of chord length at 17 AOA (P)

Fig.39 Airfoil with dimple at 40% of chord length at 17 AOA (P)
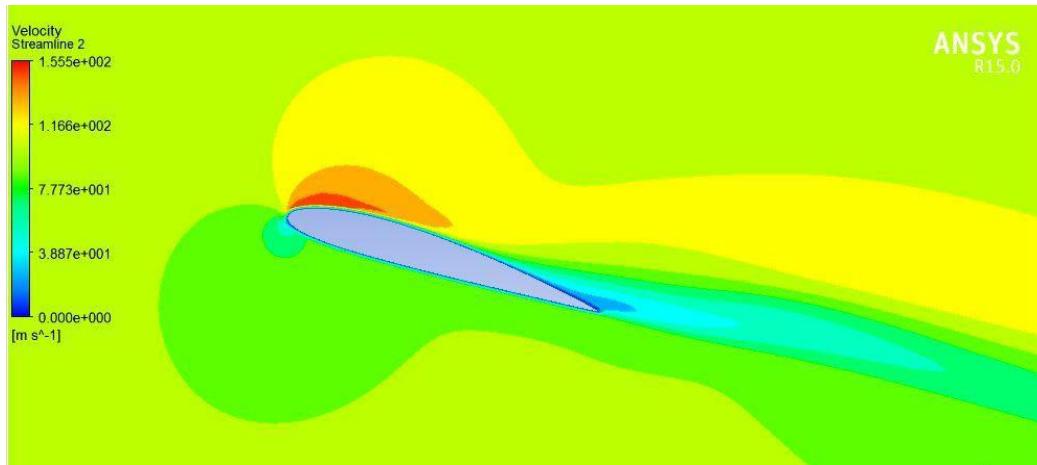
PLOTS OF VELOCITY AT 19 AOA:

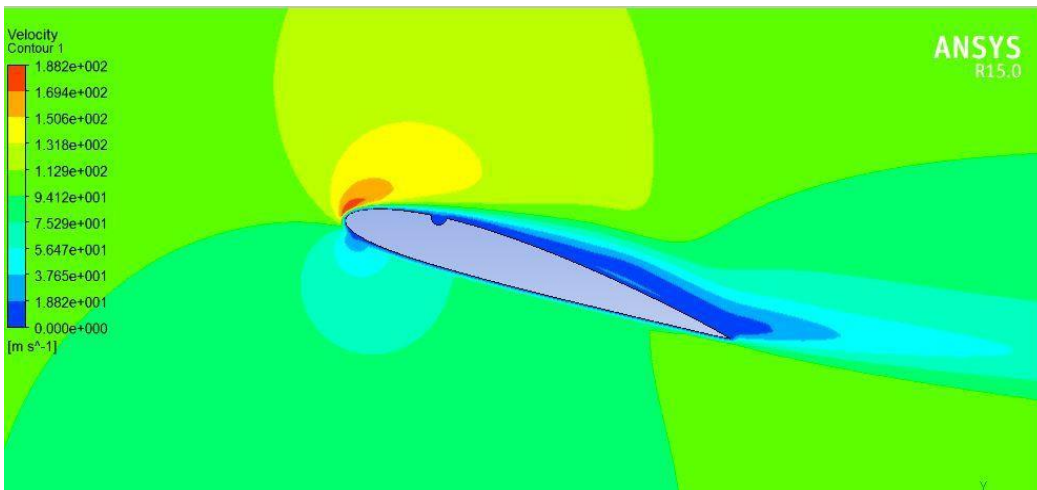Fig.40 Plain Airfoil at 19 AOA (V)

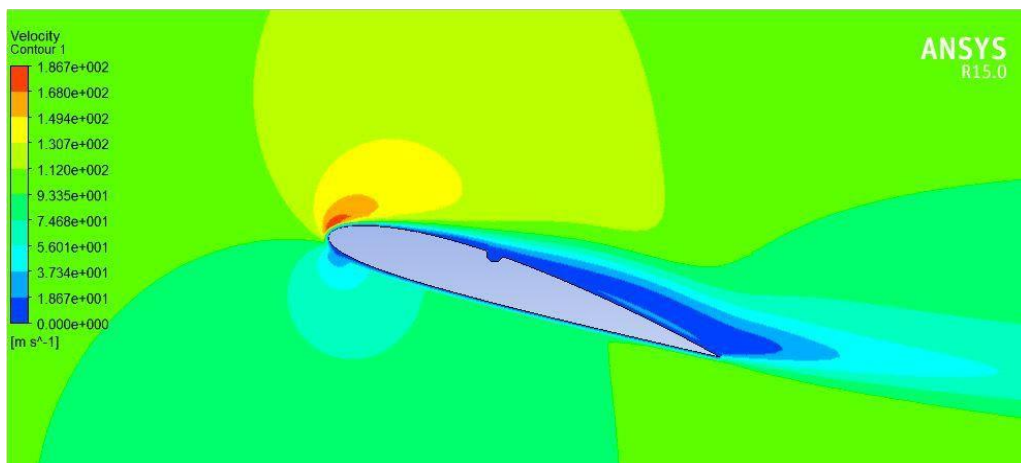Fig.41 Airfoil with dimple at 20% of chord length at 19 AOA (V)

Fig.42 Airfoil with dimple at 40% of chord length at 19 AOA (V)
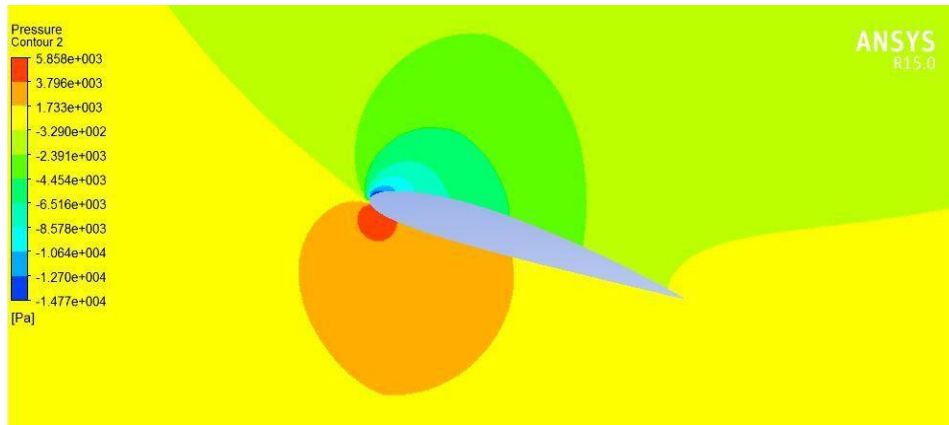
PLOTS OF STATIC PRESSURE AT 19 AOA:

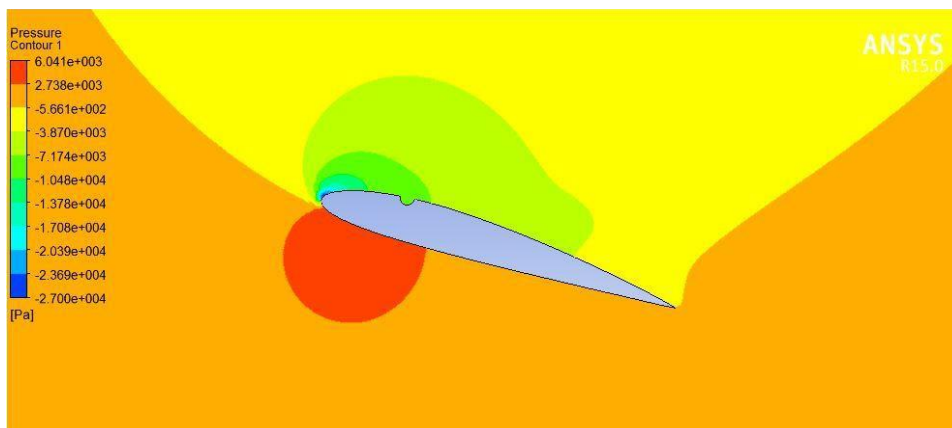Fig.43 Plain Airfoil at 19 AOA (P)

Fig.44 Airfoil with dimple at 20% of chord length at 19 AOA (P)
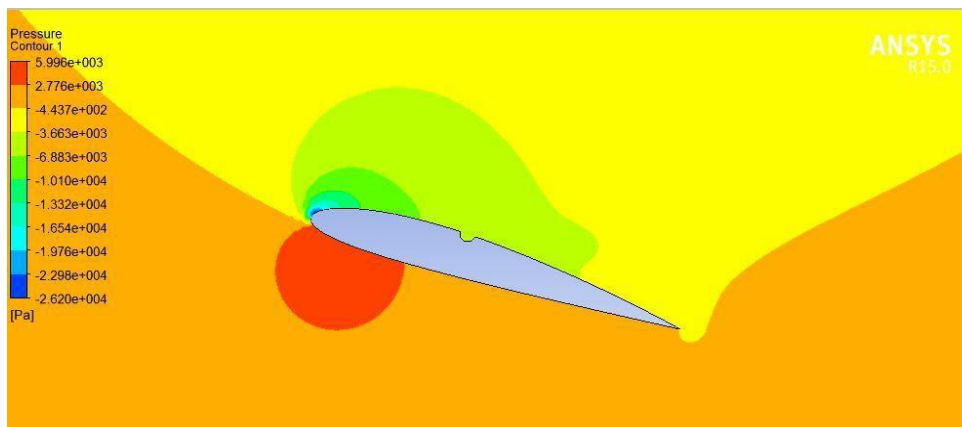

Fig.45 Airfoil with dimple at 40% of chord length at 19 AOA (P)
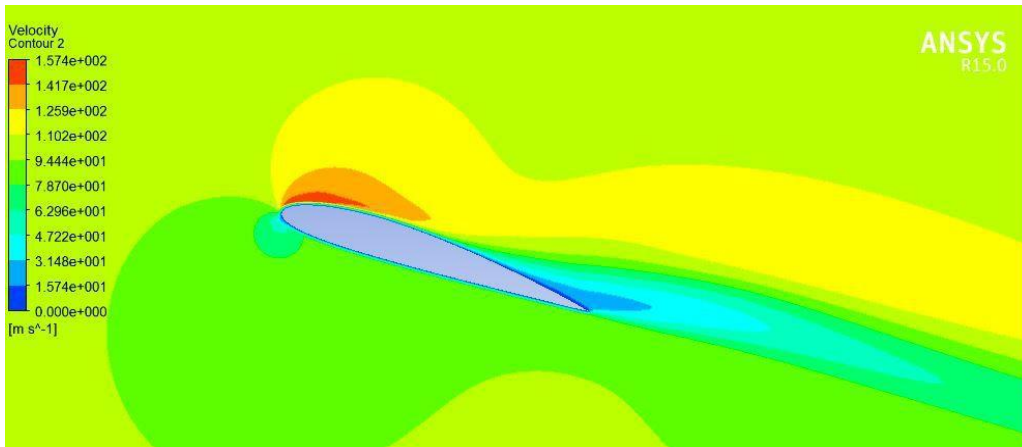
PLOTS OF VELOCITY AT 20 AOA:
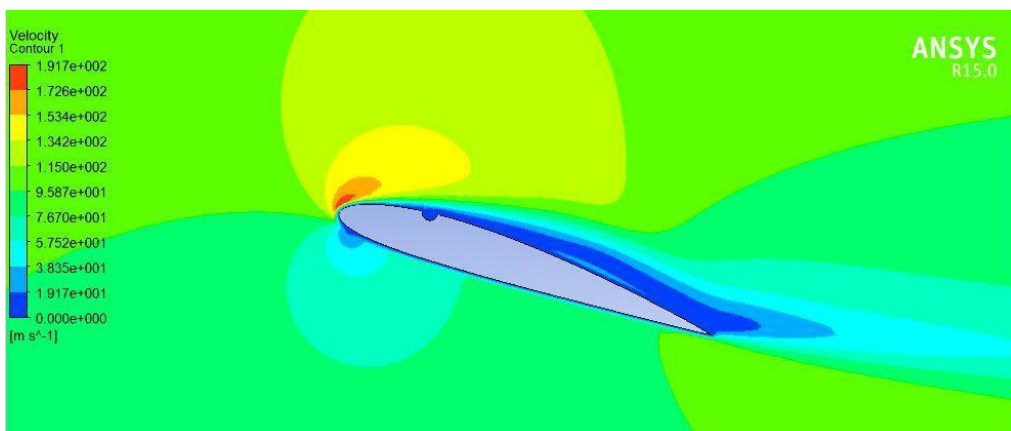

Fig.46 Plain Airfoil at 20 AOA (V)

Fig.47 Airfoil with dimple at 20% of chord length at 20 AOA (V)
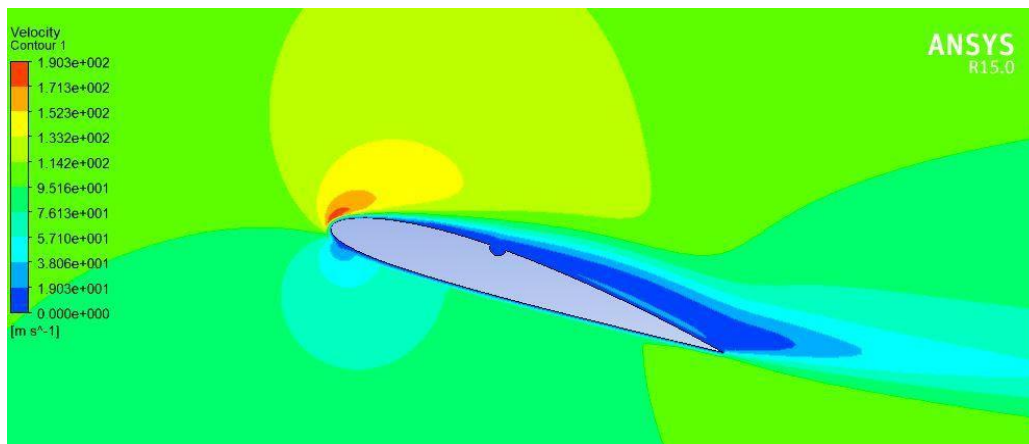

Fig.48 Airfoil with dimple at 40% of chord length at 20 AOA (V)

PLOTS OF STATIC PRESSURE AT 20 AOA:

Fig.49 Plain Airfoil at 20 AOA (P)

Fig.50 Airfoil with dimple at 20% of chord length at 20 AOA (P)

Fig.51 Airfoil with dimple at 40% of chord length at 20 AOA (P)

PLOTS OF VELOCITY AT 21 AOA:

Fig.52 Plain Airfoil at 21 AOA (V)

Fig.53 Airfoil with dimple at 20% of chord length at 21 AOA (V)

Fig.54 Airfoil with dimple at 40% of chord length at 21 AOA (V)
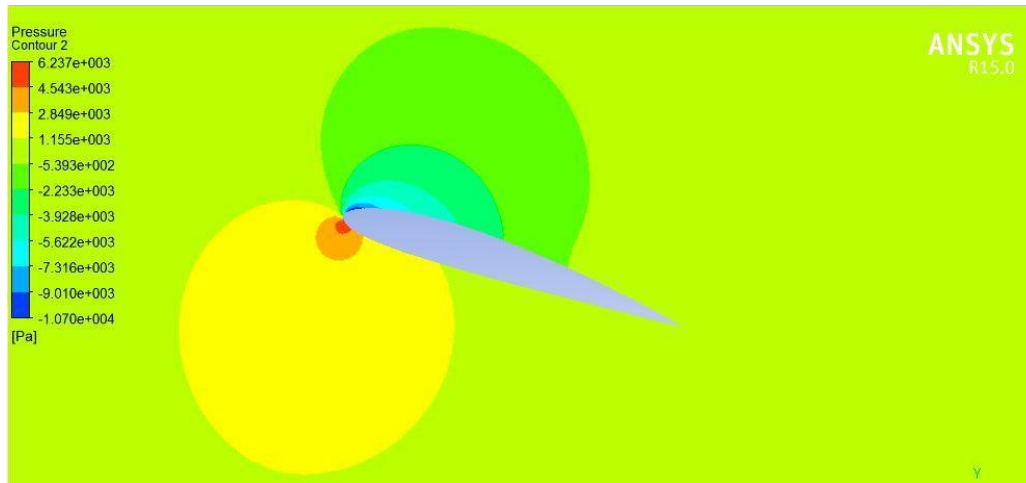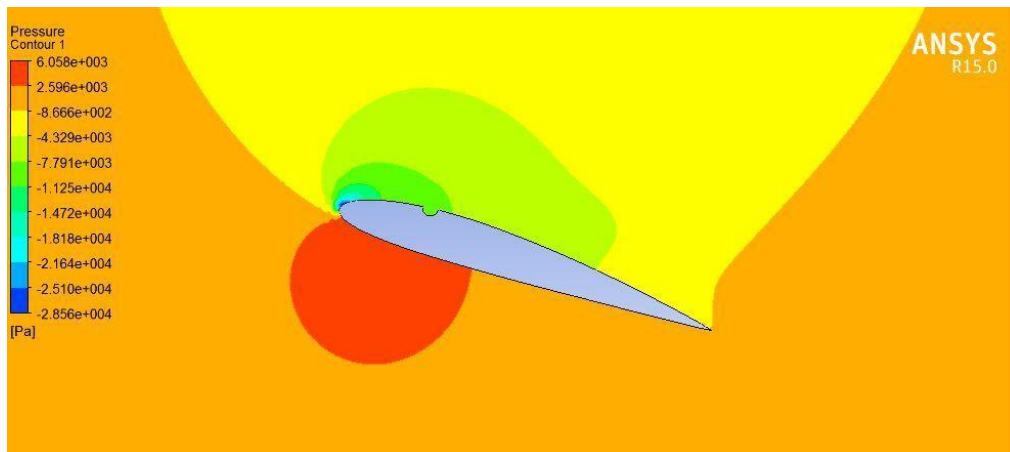
PLOTS OF STATIC PRESSURE AT 21 AOA:

Fig.55 Plain Airfoil at 21 AOA (P)

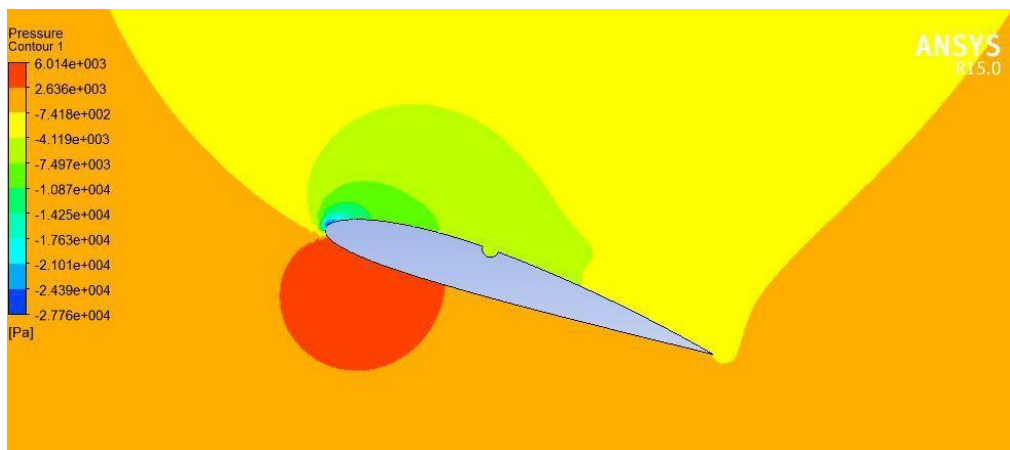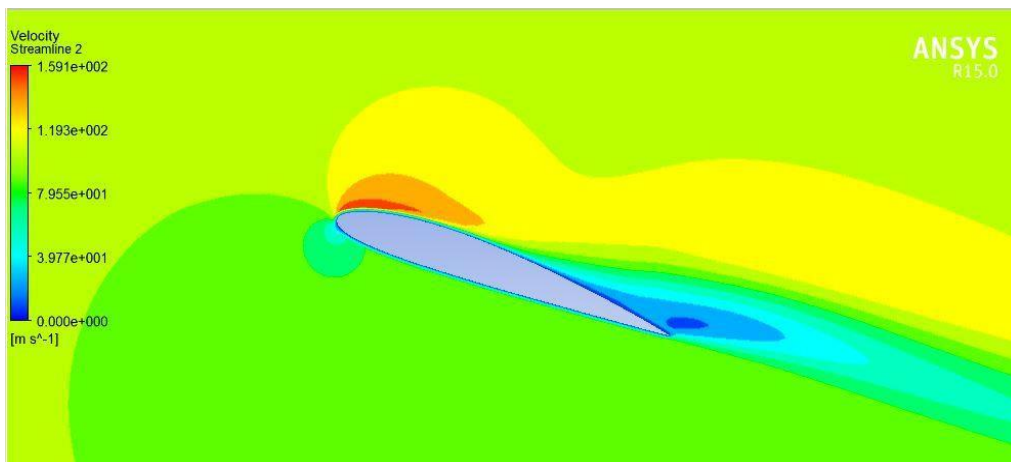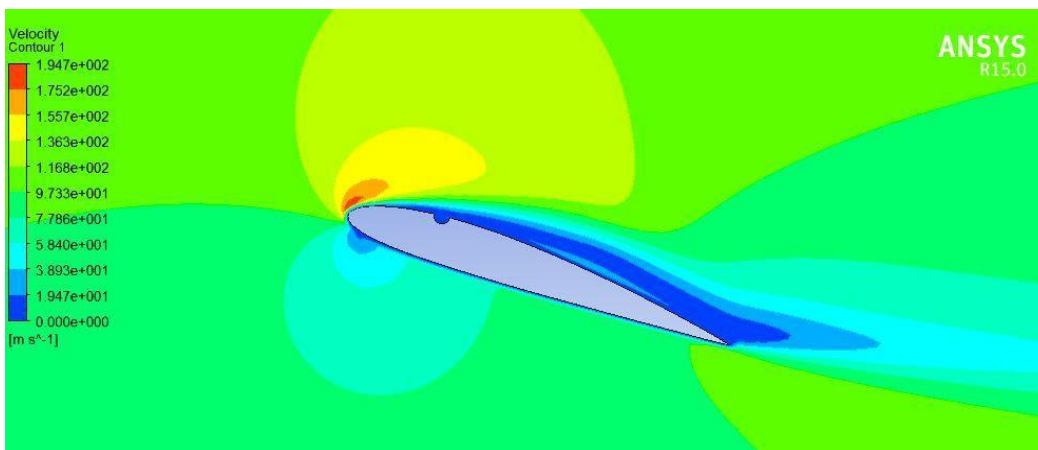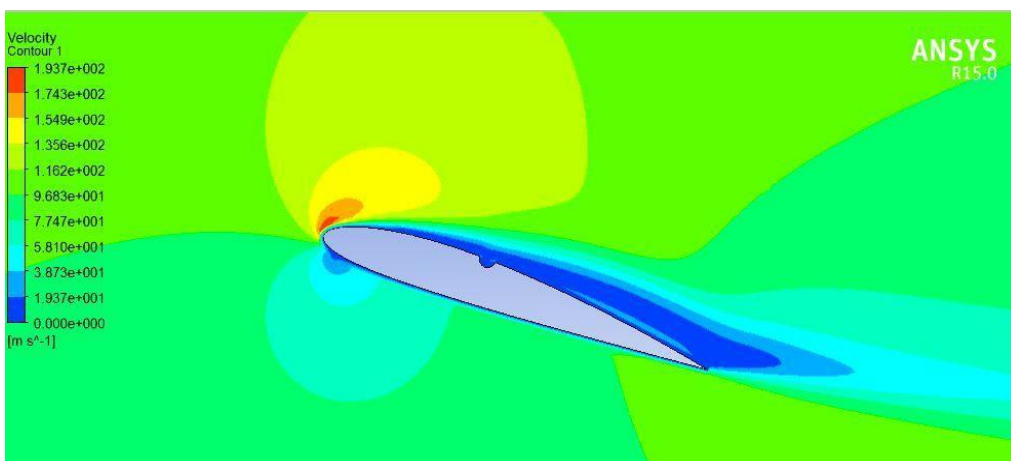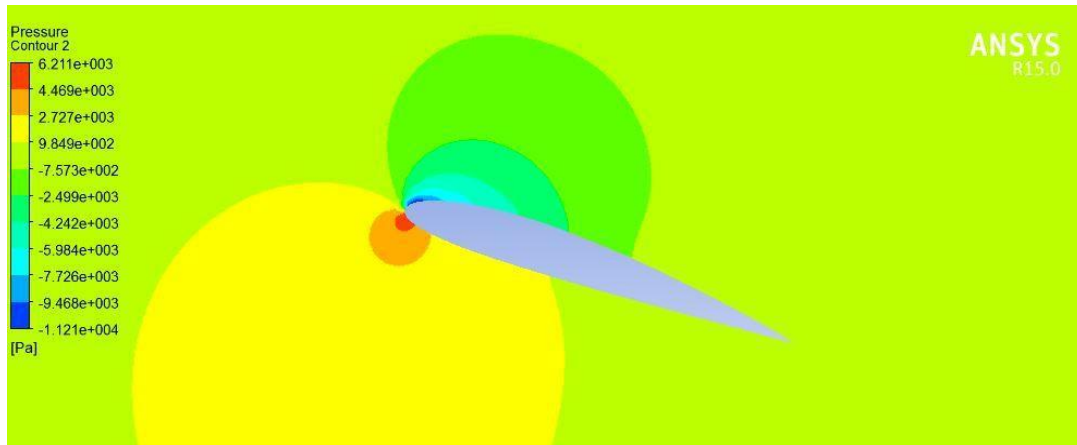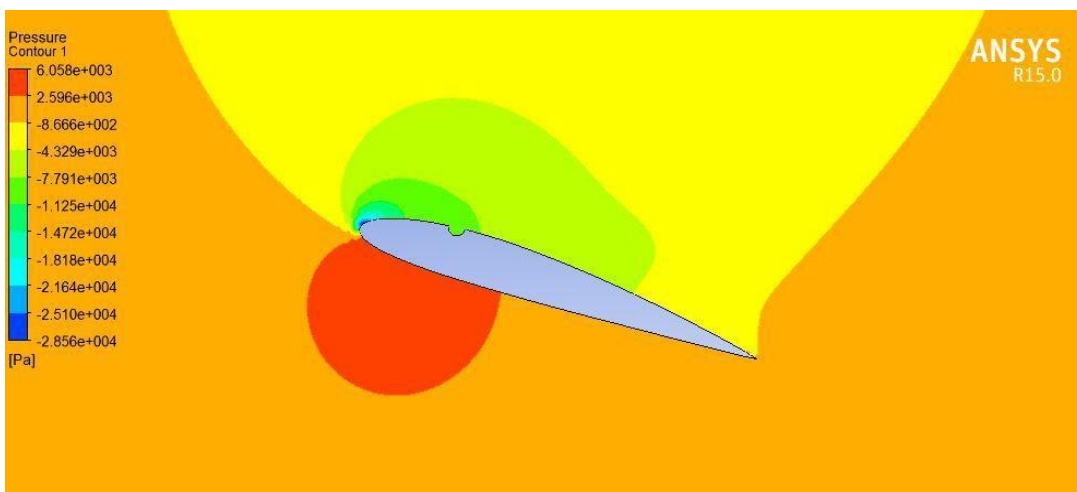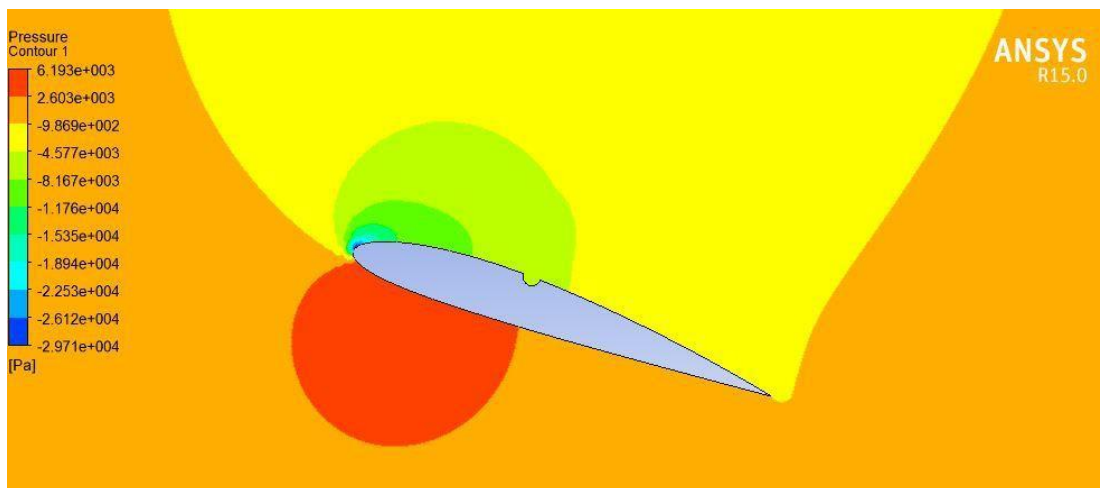Fig.56 Airfoil with dimple at 20% of chord length at 21 AOA (P)

Fig.57 Airfoil with dimple at 40% of chord length at 21 AOA (P)
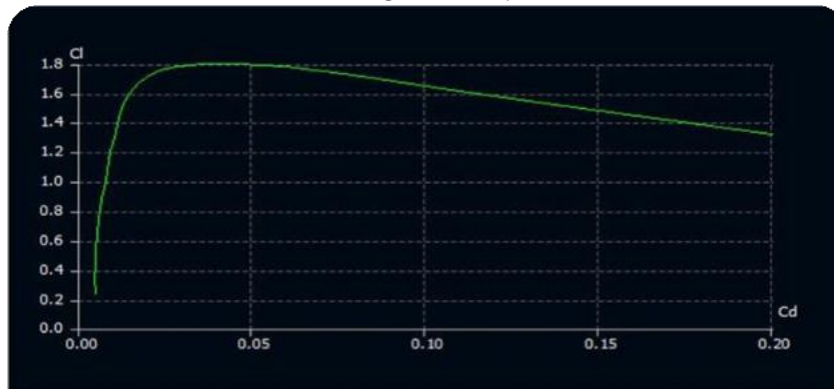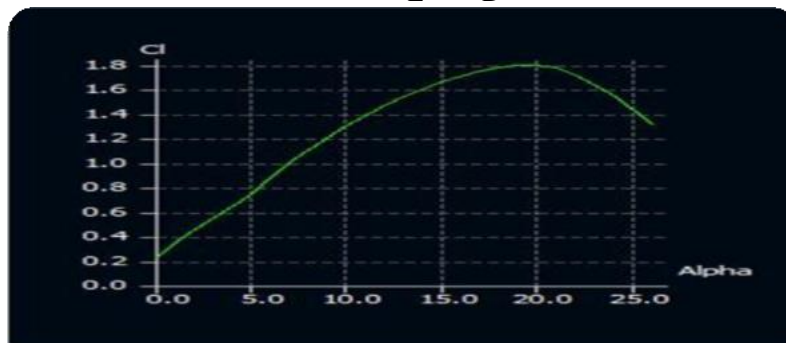
**GRAPHS
FROM XFLR:**

Fig. 58 C_L vs C_D

Fig.59 C_L vs Alpha
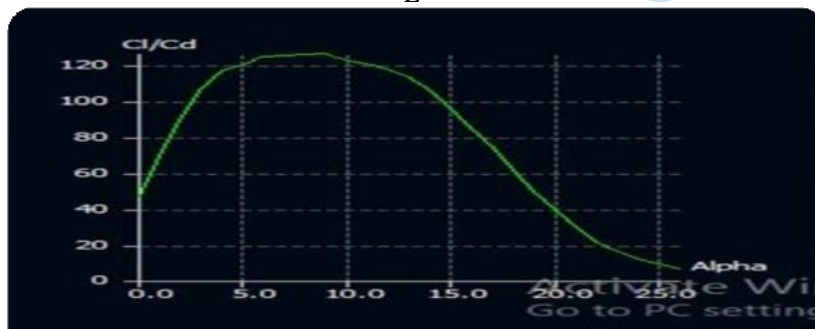
Fig. 60 C_L/C_D vs Alpha

FROM OBSERVATIONS:
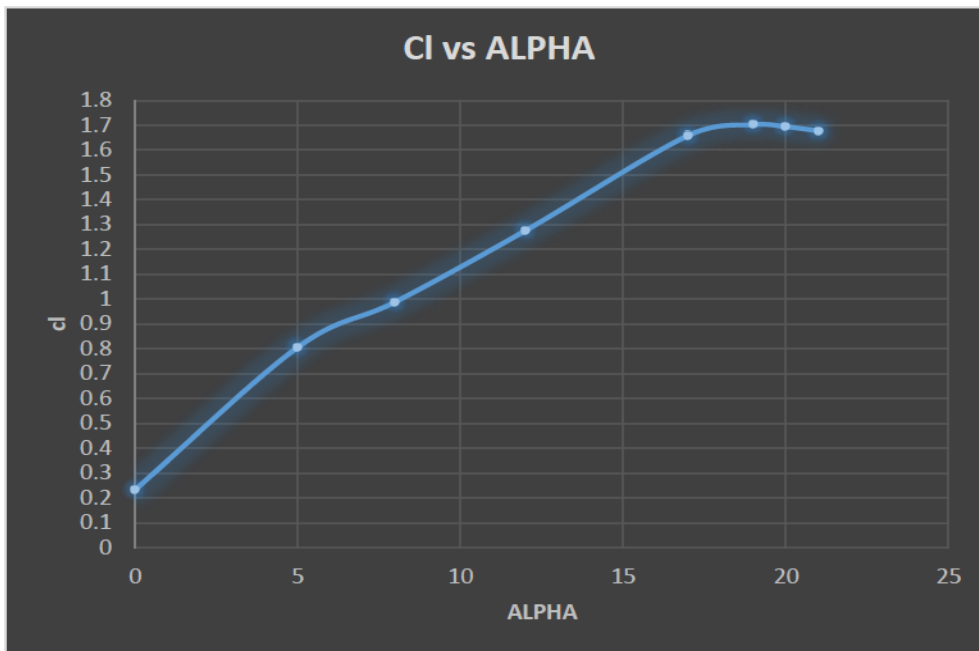
Fig .61 C$_L$ Vs Alpha
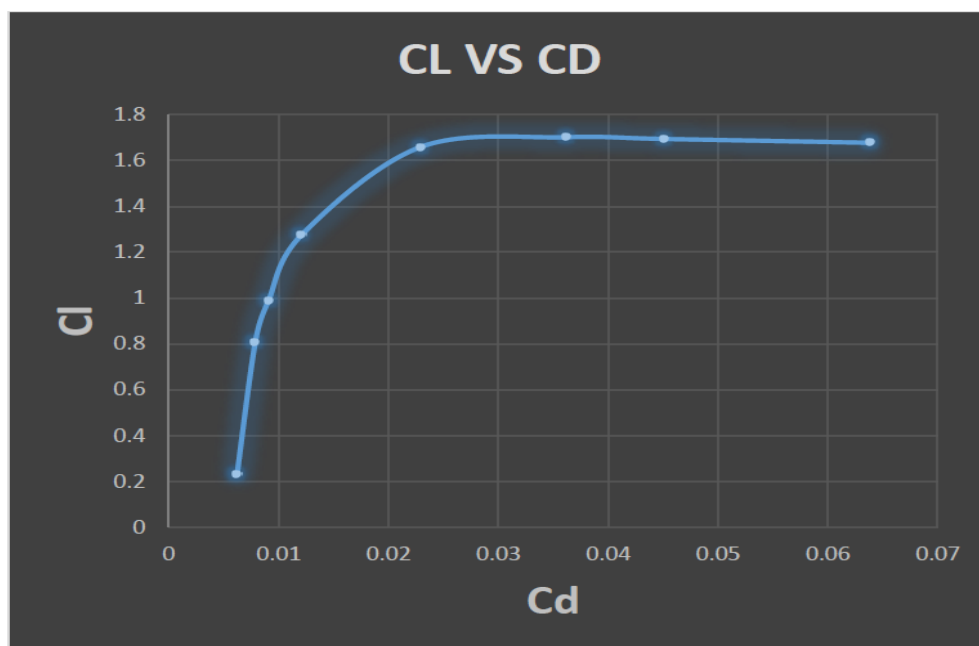
Fig. 62 C$_L$/C$_D$ Vs Alpha

V.   CONCLUSION

1. From the obtained values, it is seen that the stall angle is increased using dimples. When the flow along the surface of the airfoil enters a dimple, a small separation bubble is formed in the cavities. The consequence of the bubble formation is the acceleration of the flow between the dimples on the surface of the airfoil and boundary layer undergo a transition from laminar to turbulent. This transition leads to delay of separation of flow from the airfoil causing a substantial reduction of drag force.

2. For, plain airfoil, the stall angle is at 19 degrees. By using dimples at 20% of chord from the tip, the stall angle increases to 20 degrees but, the L/D ratio is lesser than that of the plain airfoil. When dimples are introduced at 40% of chord from the tip the stall angle increases to 21 degrees and the L/D ratio is increased to 33.79.

3. The introduction of dimples at 40% has delayed the flow separation much better than at 20% which results in significant decrease in drag.

4. A further analysis of the airfoil by changing the size of the dimple and even the shape and the location of the dimple could give a better and more accurate result of the effect of dimples.

FUTURE SCOPE OF THE PROJECT

The next step of this research could be to test the airfoils with not only different types of inward dimples, but also with outward dimples and based on how these affect the aerodynamics, the better type can be chosen, or a hybrid pattern could be tested for better efficiency.

Once these are done, the next step would be to test these patterns on a wing in actual flight conditions. This can be achieved by either the usage of inflatable surfaces on the wing to effectively change the contour of surface at specific parts for different angle of attacks by the use of pressure sensors. Or, a smart matrix of dimples can be created which will arrange itself over the airfoil by sensing the boundary layer separation at different points. This sensing of boundary layer separation will be done through MEMS based pressure sensors which will estimate the pressure gradient. Through a predefined algorithm using this data for MEMS pressure sensors boundary layer separation can be predicted. The same algorithm will then send a command to rearrange the dimple matrix to optimize for maximum aerodynamic efficiency.
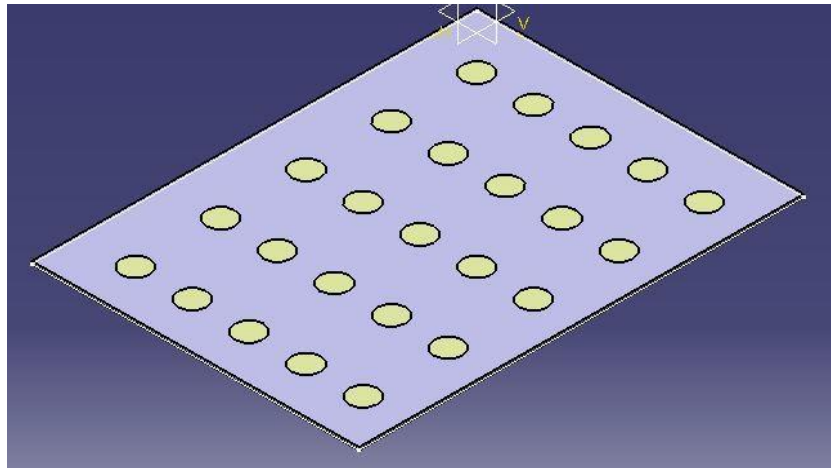

Fig. 63 Inflatable surfaces

Fig.64 Multi dimpled matrix configuration

REFERENCES

[1]. Hossain, Md. Amzad & Uddin, Md & Mustak, Rubiat & Mashud, Mohammad. (2015). Experimental study of aerodynamic characteristics of airfoils using different shaped dimples. 4. 13-17.

[2]. Steger J, Benek J. On the use of composite grid schemes in computational aerodynamics. Computer Methods in Applied Mechanics and Engineering. 1987;64(1-3):301-320.

[3]. Mehta R. Aerodynamics of Sports Balls. Annual Review of Fluid Mechanics. 1985;17(1):151-189.

[4]. 4. Asai T, Ito S, Seo K, Hitotsubashi A. Fundamental aerodynamics of a new volleyball. Sports Technology. 2010;3(4):235-239.

[5]. Alam F, Chowdhury H, Moria H, Steiner T and Subic A. A Comparative Study of Golf Ball Aerodynamics. Proceedings of the 17th Australasian Fluid Mechanics Conference (AFMC) 2010; 5-9 December, Auckland.

[6]. C.E. Smith, N. Beratlis, E. Balaras, K. Squires, M. Tsunoda Numerical investigation of the flow over a golf ball in the subcritical and supercritical regimes International Journal of Heat and Fluid Flow, 31 (2010), pp. 262-273.

[7]. Smits AJ and Ogg S. Golf Ball Aerodynamics. In: J.M. Pallis, R. Mehta, M. Hubbard, Editors, Proceedings 5th International Sports Engineering Conference, 2004.

[8]. BRIAN F M. Golf balls with isodiametrical dimples. United States of America; US5377989, 2019.

[9]. Livya, E., Ganna Anitha and P. Valli. "Aerodynamic Analysis of Dimple Effect on Aircraft Wing." (2015).

[10]. 5. Arunkumar A, Gowthaman T, Muthuraj R, Vinothkumar S, Balaji K. Numerical Investigation over Dimpled Wings of an Aircraft. International Journal for Research in Applied Science and Engineering Technology. 2017; V(IV):206-211.

[11]. Bhadri R, Tej R, Srinath S. Aerodynamic effect on Dimple on Aircraft Wings. International conference on advance in Mechanical,Aeronautical and Production Techniques, MAPT 2011.

[12]. Al-Obaidi, Abdulkareem Sh & Soh, Zheng. (2016). Numerical Analysis of the Shape of Dimple on the Aerodynamic Efficiency of NACA 0012 Airfoil.

[13]. Mustak, Rubiat & Uddin, Md & Mashud, Mohammad. (2018). Effect of Different Shaped Dimples on Airfoils.